

Compact Optical 3R Regeneration Using a Traveling-Wave Electroabsorption Modulator

Hsu-Feng Chou, Zhaoyang Hu, John E. Bowers, *Fellow, IEEE*, and Daniel J. Blumenthal, *Fellow, IEEE*

Abstract—We propose and demonstrate a novel reamplification, retiming, and reshaping regeneration approach that utilizes the photocurrent signal and the nonlinear electrooptical transfer function of a traveling-wave electroabsorption modulator in an electrical ring oscillator. All the required functionalities such as clock recovery, pulse generation, and nonlinear decision are implemented with the same device, leading to a very compact configuration. In addition, wavelength conversion and electrical signal monitoring can be realized at the same time. With a degraded 10-Gb/s return-to-zero input, 1.0 dB of negative power penalty and 50% timing jitter reduction are measured after regeneration.

Index Terms—Clock recovery, electroabsorption modulator (EAM), regeneration, traveling-wave (TW), wavelength conversion.

I. INTRODUCTION

TO EXTEND the reach of ultralong-haul transmission and to increase the scalability of all-optical networks, reamplification, retiming, and reshaping (3R) regeneration techniques are required to restore accumulated impairments in both the amplitude and the time domains. Architectures based on nonlinearities in fibers, semiconductor optical amplifiers (SOAs), and electroabsorption modulators (EAMs) have been demonstrated recently [1]–[5]. Reamplification of optical signals using the erbium-doped fiber amplifier (EDFA) is a well-known success in various transmission systems. An alternative is the SOA, which offers very compact reamplification due to its small size and integration potential. However, the pattern dependence of SOA originating from the gain recovery dynamics is a major challenge in practical application. On the other hand, in order to retime and reshape return-to-zero (RZ) signals, three functionalities must be implemented. First, *clock recovery* from the degraded signal is necessary to acquire synchronization with a reduced jitter, which is often realized with the aid of electronics. The recovered electrical clock then drives an *optical pulse source* to generate a clean pulse train, which provides retiming and lateral reshaping. Finally, the generated pulse train is modulated by a *nonlinear decision gate* controlled by the degraded signal, where vertical reshaping is obtained. By implementing the three functionalities individually, effective 3R regenerations can be realized [1], [2] but many components are required. Incorporating some of these functionalities together

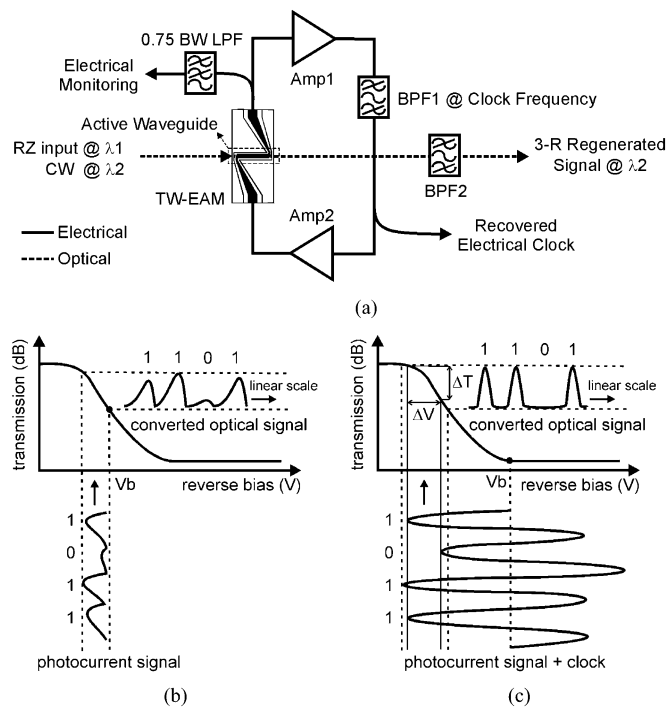


Fig. 1. (a) Configuration of the compact PAW-Regeneration. (b) E-O transformation in the TW-EAM without an electrical clock and (c) with an electrical clock.

with fewer components would be advantageous. For example, an EAM can work both as a phase comparator for clock recovery and a nonlinear decision gate [4]. A self-pulsating laser can recover an optical sinusoidal pulse train, combining clock recovery and an optical pulse source [5].

In this letter, we propose a compact 3R approach that incorporates all three functions for retiming and reshaping with a traveling-wave EAM (TW-EAM) [6]. This 3R regeneration is based on the photocurrent-assisted wavelength conversion (PAW-Conversion) [7], [8] and is called PAW-Regeneration. In addition, simultaneous clock recovery is realized by setting the TW-EAM in an electrical ring oscillator [9]. 3R regeneration of 10-Gb/s RZ data is demonstrated.

II. PRINCIPLE OF PAW-REGENERATION

The configuration of PAW-Regeneration is schematically shown in Fig. 1(a), where the core is PAW-Conversion inside the TW-EAM [7]. Conventionally, absorption saturation due to a strong input signal is used to achieve wavelength conversion and is the enabling mechanism for many 3R regenerators [2], [4]. However, it is not absolutely necessary for the proposed

Manuscript received July 12, 2004; revised October 6, 2004. This work was funded by Defense Advanced Research Projects Agency (DARPA)/MTO under CS-WDM Grant N66001-02-C-8026

The authors are with the Department of Electrical and Computer Engineering, University of California, Santa Barbara, Santa Barbara, CA 93106-9560 USA (e-mail: Hsu-Feng.Chou@ieee.org).

Digital Object Identifier 10.1109/LPT.2004.839453

PAW-Regeneration and the following discussion will only focus on the photocurrent-assisted mechanism. Nevertheless, many of these arguments can also be applied to the saturation mechanism.

When the optical input signal at λ_1 enters the reverse-biased TW-EAM, it gets absorbed quickly within a short distance and generates photocurrent signals propagating along both directions of the traveling-wave electrodes. When the copropagating tributary goes through the rest of the active waveguide, it modulates the local voltage and changes the absorption experienced by the continuous wave (CW) at λ_2 . As a result, wavelength conversion from λ_1 to λ_2 is realized. This photocurrent signal can subsequently be detected by outside electronics, providing electrical monitoring capability. The counterpropagating tributary is not utilized in the presented configuration and is terminated at the output of a microwave amplifier (Amp2).

One important feature of PAW-Regeneration is that it can mitigate the bandwidth requirement for TW-EAM in RZ signal regeneration. The response of the TW-EAM as a photodetector may not be fast enough to resolve the pulse shape and causes distortions such as a long falling tail in the photocurrent signal. As shown in Fig. 1(b), the converted signal carries essentially the same distortion, resulting in excess power penalty. This problem is solved in PAW-Regeneration by supplying a synchronized electrical clock to the TW-EAM [8]. As shown in Fig. 1(c), the photocurrent signal adds with a stronger sinusoidal clock and the long tails are pulled down. This process also suppresses the noise between bits. The shape and timing of the converted signal are mainly determined by the sinusoidal clock while information is transferred from the input by the photocurrent signal. As a result, *retiming* and *lateral reshaping* are obtained.

Vertical reshaping is realized by utilizing the nonlinear electrooptical (E-O) transfer function of the TW-EAM. Fig. 1(c) shows that by setting the bias voltage properly, the mark levels can fall in a smooth region on the transfer curve and noise in the mark can be compressed after E-O transformation. On the other hand, as long as the electrical eye opening, ΔV , is large enough so that the extinction ratio of the converted signal ΔT is better than that of the degraded input, noise in the space can be suppressed in the converted signal. In other words, vertical reshaping is achieved by redistributing noise through the nonlinear E-O transformation.

To realize a more compact regenerator, *clock recovery* is incorporated into PAW-Regeneration by constructing a ring oscillator [9] that is composed of the TW-EAM, two microwave amplifiers (Amp1 and Amp2), and a bandpass filter (BPF1), as depicted in Fig. 1(a). The spectrum of the photocurrent signal contains a clock tone at the bit rate, which can be utilized for injection-locking the ring oscillator. Due to the spectral purity of the ring oscillator, the recovered electrical clock is synchronized with the pump signal but with a reduced jitter, providing a reference for retiming. Thus, a compact and self-sustained 3R regeneration is completed.

III. EXPERIMENT

The proposed concept is demonstrated at 10 Gb/s. The electrical ring oscillator has approximately 4.7 dB of small-signal

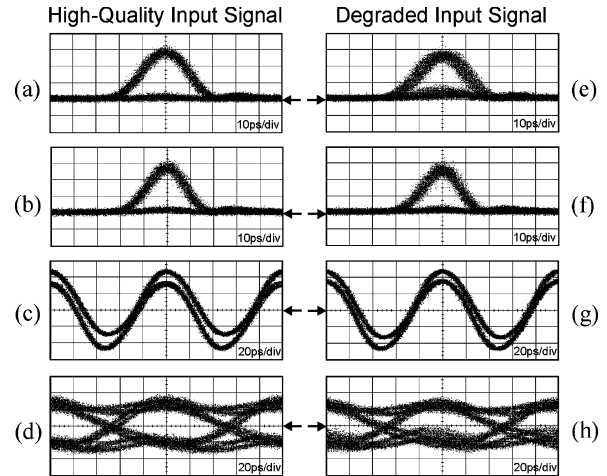


Fig. 2. Eye diagrams of (a), (e) input signal, (b), (f) wavelength converted signal, (c), (g) monitored electrical signal without LPF, and (d), (h) with LPF. The arrows indicate zero levels.

gain. At resonance, it is arranged so that only Amp1 saturates, preventing waveform distortion due to saturation of Amp2, which drives the TW-EAM. In order to maintain signal integrity, the reflection of photocurrent signals from outside electronics is kept lower than -20 dB up to 10 GHz by using additional attenuators. BPF1 has a 100-MHz bandwidth, centered at 9.953 GHz. The loop of the oscillator is approximately 0.75 m long and the corresponding free-spectral range is 533 MHz. As a result, only one resonance mode is picked by BPF1. An electrical phase shifter is inserted in the loop to tune the resonance frequency. The RZ input signal is a 15-dBm 20-ps $2^31 - 1$ pseudorandom binary sequence (PRBS) data at 1550.92 nm. The CW is 4 dBm at 1557.50 nm. EDFAs are used for reamplification.

First, the regenerator is evaluated with a high-quality input signal [Fig. 2(a)] in order to access the back-to-back performance. The extinction ratio of the high-quality input signal is over 15 dB. The locking range is 2.3 MHz, within which the relative phase of the oscillating clock and the photocurrent signal can be adjusted by the phase shifter to optimize the converted signal. The bias voltage of the TW-EAM is -3.0 V and the strength of the oscillating clock at the input of the TW-EAM is 5.4 Vpp. The converted eye [Fig. 2(b)] is clean and has a smaller width of 15 ps, which shows lateral reshaping. The extinction ratio of the converted signal is higher than 10 dB. Bit-error-rate (BER) results in Fig. 3 show that only 0.3 dB of power penalty is imposed. Timing jitter is measured by integrating the single-sideband noise from 1 kHz to 10 MHz with a 100-Hz resolution bandwidth. The jitter of the input signal, the recovered electrical clock, and the converted signal are 727, 349, and 590 fs, respectively, showing retiming capability of the regenerator. Fig. 2(c) shows the monitored electrical signal without filtering, which is a combination of the photocurrent signal and the oscillating clock. With a 7.5-GHz low-pass filter (LPF), the clock tone can be suppressed and a nonreturn-to-zero signal is obtained as in Fig. 2(d), which gives error-free BER measurement and provides electrical monitoring.

Next, the input signal is intentionally degraded [Fig. 2(e)]. The timing jitter is increased by applying a 2-MHz frequency

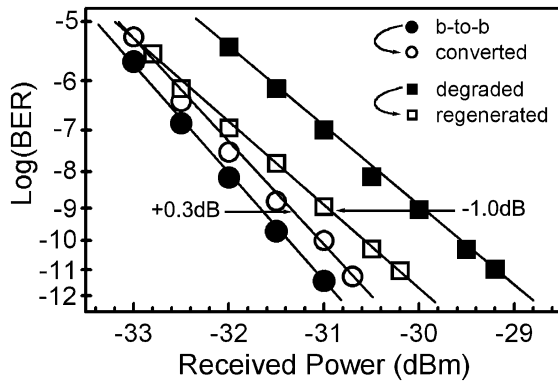


Fig. 3. BER measurements with high-quality (back-to-back) and degraded input signals.

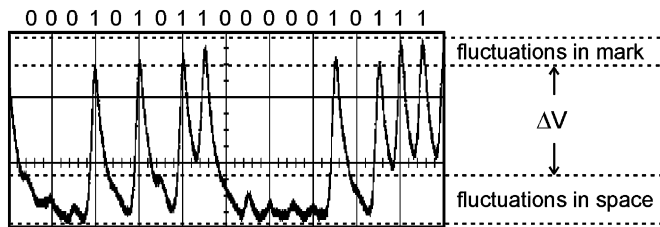


Fig. 4. Bit pattern of a 15-dBm, $2^7 - 1$ PRBS, high-quality input signal detected by the TW-EAM at -3.0 -V bias. (200 ps/div).

modulation to the pulse source with a 0.15 modulation index. The extinction ratio is decreased to about 6 dB by lowering the driving voltage to the transmitter and a change in modulator bias. Other parameters such as the input power and the TW-EAM bias are kept the same. After regeneration, the converted eye [Fig. 2(f)] shows a reduced jitter, an increased extinction ratio, and a shortened pulsewidth. A 1.0-dB negative power penalty is measured, as shown in Fig. 3. The jitter of the input signal, the recovered electrical clock, and the converted signal are 2.9, 1.2, and 1.5 ps, respectively, showing up to 50% timing jitter reduction. ΔV in Fig. 2(g) is smaller than that in the previous case due to the degraded extinction ratio of the input signal but after E-O transformation the extinction ratio can still be improved to over 10 dB. The above results verify successful operation of the compact 3R PAW-Regeneration.

IV. DISCUSSION

The required input power may depend on several factors such as the degree of degradation, the response, and the transfer function of the TW-EAM. A high modulation efficiency (decibels per volts) is needed to keep the required ΔV low, which implies a lower input power. From Fig. 2(c), it is estimated that ΔV is 0.4 V inside the TW-EAM, taking into account that the impedance of the active waveguide is only 25 Ω . This corresponds to 6 dB of extinction ratio with a 15-dB/V modulation efficiency. However, the extinction ratio of the converted signal is over 10 dB, indicating that the saturation mechanism works in favor of PAW-Regeneration in the experiment. A limiting factor of PAW-Regeneration is the speed of the TW-EAM as a photodetector (currently 12 GHz). Fig. 4 shows the bit pattern of the RZ input detected by the TW-EAM at -3.0 V of bias in the

absence of the oscillating clock. The PRBS length is reduced to $2^7 - 1$ so that the oscilloscope can show the trace properly. As shown in Fig. 4, in addition to the long falling tails, which can be counter-acted by the electrical clock, a limited bandwidth can cause pattern-dependent fluctuations in the mark and the space, leading to a reduced ΔV . To increase the operation speed and ΔV , the carrier escape time from the quantum wells should be improved. An alternative approach is to combine a separate high-speed photodetector with the TW-EAM [10]. Furthermore, hybrid integration of the TW-EAM and associated electronics [11] can lead to an even more compact PAW-Regeneration.

V. CONCLUSION

A very compact 3R PAW-Regeneration with electrical monitoring capability is proposed and demonstrated, which incorporates all required functionalities into a single TW-EAM. Clock recovery is realized by injection-locking a ring oscillator with the clock tone in the photocurrent signal. An optical pulse source and a nonlinear decision gate are merged together in the TW-EAM by using the recovered clock and the nonlinear E-O transformation. 3R regeneration is demonstrated with a reduced timing jitter and a negative power penalty.

REFERENCES

- [1] O. Leclerc, B. Lavigne, E. Balmefrezol, P. Brindel, L. Pierre, D. Rouvillain, and F. Seguin, "Optical regeneration at 40 Gb/s and beyond," *J. Lightw. Technol.*, vol. 21, no. 11, pp. 2779–2790, Nov. 2003.
- [2] T. Otani, T. Miyazaki, and S. Yamamoto, "40-Gb/s optical 3R regenerator using electroabsorption modulators for optical networks," *J. Lightw. Technol.*, vol. 20, no. 2, pp. 195–200, Feb. 2002.
- [3] J. Leuthold, B. Mikkelsen, R. E. Behringer, G. Raybon, C. H. Joyner, and P. A. Besse, "Novel 3R regenerator based on semiconductor optical amplifier delayed-interference configuration," *IEEE Photon. Technol. Lett.*, vol. 13, no. 8, pp. 860–862, Aug. 2001.
- [4] E. S. Awad, P. S. Cho, C. Richardson, N. Moulton, and J. Goldhar, "Optical 3R regeneration using a single EAM for all-optical timing extraction with simultaneous reshaping and wavelength conversion," *IEEE Photon. Technol. Lett.*, vol. 14, no. 9, pp. 1378–1380, Sep. 2002.
- [5] C. Bornholdt, J. Slovak, and B. Sartorius, "Semiconductor-based all-optical 3R regenerator demonstrated at 40 Gbit/s," *Electron. Lett.*, vol. 40, pp. 192–193, Feb. 2004.
- [6] Y.-J. Chiu, H.-F. Chou, V. Kaman, P. Abraham, and J. E. Bowers, "High extinction ratio and saturation power traveling-wave electroabsorption modulator," *IEEE Photon. Technol. Lett.*, vol. 14, no. 6, pp. 792–794, Jun. 2002.
- [7] H.-F. Chou, Y.-J. Chiu, A. Keating, J. E. Bowers, and D. J. Blumenthal, "Photocurrent-assisted wavelength (PAW) conversion with electrical monitoring capability using a traveling-wave electroabsorption modulator," *IEEE Photon. Technol. Lett.*, vol. 16, no. 2, pp. 530–532, Feb. 2004.
- [8] H.-F. Chou, J. E. Bowers, and D. J. Blumenthal. Novel photocurrent-assisted wavelength (PAW) converter using a traveling-wave electroabsorption modulator with signal monitoring and regeneration capabilities. presented at Optical Fiber Communication Conf. [CD-ROM] Paper FD4
- [9] Z. Hu, H.-F. Chou, J. E. Bowers, and D. J. Blumenthal, "40-Gb/s optical clock recovery using a compact traveling-wave electroabsorption modulator-based ring oscillator," *IEEE Photon. Technol. Lett.*, vol. 16, no. 5, pp. 1376–1378, May 2004.
- [10] T. Yoshimatsu, S. Kodama, K. Yoshino, and H. Ito, "100 Gbit/s error-free retiming operation of monolithic optical gate integrating with photodiode and electroabsorption modulator," *Electron. Lett.*, vol. 40, pp. 626–628, May 2004.
- [11] Z. Hu, B. Liu, X. Yang, J. E. Bowers, and D. J. Blumenthal. All-Optical 40 Gb/s cross-wavelength transferred clock-recovery for 3R wavelength conversion using a traveling-wave electroabsorption modulator-based resonant cavity. presented at Optical Fiber Communication Conf. [CD-ROM] Paper WD3